Size-dependent hot-electron dynamics in small Pd_n^--clusters

N. Pontius, G. Lüttgens, P. S. Bechthold, M. Neeb, and W. Eberhardt
Institut für Festkörperforschung, Forschungszentrum Jülich GmbH, D-52425 Jülich, Germany

(Received 16 July 2001; accepted 11 September 2001)

Using time-resolved photoelectron spectroscopy we show that electron relaxation processes via inelastic electron–electron scattering are efficient energy dissipation channels not only in bulk metals but also in extremely small transition metal clusters. The photoelectron spectra of optically excited Pd_3^-, Pd_4^-, and Pd_7^- reveal effective electron relaxation times of less than 100 fs. Moreover the relaxation times vary with cluster size. In comparison to simple metal clusters the bulklike inelastic scattering rates in open *d*-shell transition metal clusters are attributed to the larger valence electron level density. An energy transfer to the vibrational degrees of freedom occurs within 10 ps. [DOI: 10.1063/1.1415449]

I. INTRODUCTION

The combination of femtosecond light pulses with the pump–probe technique permits to study ultrashort electron dynamics in metallic systems in real time. Of special interest is the dynamics of excited electrons in a nonequilibrium state, which is created when an electron is photoexcited by an ultrashort light pulse. Optical excitations in transition metals have extremely short lifetimes, usually much less than 100 fs.[1–4] These high inelastic scattering rates result from strong electron–electron interactions as described by Fermi liquid theory.[5,6]

Generally, the probability of inelastic electron scattering depends on the level density of occupied and unoccupied states around the Fermi level. Compared to bulk metals the electronic level density in clusters is discrete rather than continuous due to quantum confinement. Therefore ultrafast electron relaxation processes are usually not feasible in small clusters. This is definitely true for simple metal clusters where the valence orbitals are derived from *s/p*-states only. Therefore photoexcited states in small simple and noble metal clusters are usually long-lived with respect to a vibrational period. In contrast, the level density of open *d*-shell metal clusters is distinctly larger due to a considerable mixing of *d*-orbitals in the valence region making inelastic electron scattering processes more probable than in simple metal clusters. For example, in a four-atomic transition metal cluster additionally 40 *d*-levels exist within a bandwidth of 4–5 eV around the Fermi level. Note that the orbital-band width rapidly approaches the bulk value because the maximum orbital interaction results from the orbital overlap of nearest neighbor atoms, e.g., as confirmed for Ni_4 and Pt_{13}.[7] Thus the small *d*-band width implies a mean level spacing of only about 100 meV, which is distinctly smaller than that of a tetra-atomic simple metal cluster. Moreover, taking into account the vibrational sublevels, which have vibrational energies of usually less than 100 meV, the total energy level density converges rapidly towards a fairly dense distribution as exhibited in the photodetachment spectra of small transition metal clusters.[8,9] Due to partially filled *d*-orbitals the high level density extends some eV above the highest occupied molecular orbital (HOMO). At higher energies, the unoccupied level density is strongly reduced as it is mainly composed from hybridized s/p-orbitals having a band width of more than a Rydberg.

As the valence electronic structure is a characteristic property of every cluster we expect the relaxation times to be strongly dependent on the size of the cluster. Size-dependent electron relaxation times have recently been observed for matrix-isolated Ag-nanoparticles of less than 5 nm radius ($\sim 10^5$ atoms).[10–12] This size dependence has been explained by a reduced dynamic screening induced by both electron spillout and spatial *d*-electron localization in Ag-nanoparticles as quantitatively deduced from the jellium model.[13–15] Within this approach the electron thermalization times decrease continuously with decreasing particle size starting with the bulk value in agreement with the experimental observation.[11] As the discretization of the electronic structure can no longer be neglected, this approach, which has been extrapolated from the bulk surface, is certainly not suitable to predict the relaxation times for small clusters with less than 1 nm diam. Indeed, we here show by pump–probe photoelectron spectroscopy that the relaxation times of Pd_3^-, Pd_4^-, and Pd_7^- depend in a nonmonotonic manner on the size of the clusters due to distinct differences in the electronic structure.

II. EXPERIMENT

The experimental setup has been described in detail in Ref. 16. Briefly, the clusters are produced by laser vaporization of a metal rod and subsequent condensation and cooling in a pulsed He-carrier gas. Cluster anions are mass-selected by a time-of-flight mass spectrometer. Upon entering a time-of-flight electron spectrometer,[17] an electron is detached from the mass-selected cluster anion via pump–probe photoelectron spectroscopy with two subsequent, orthogonally polarized infrared femtosecond laser pulses ($\sim$80 fs, 50 Hz, $\sim$5 mJ/cm^2). An electron kinetic energy resolution of $\approx$100 meV at 1 eV has been measured.

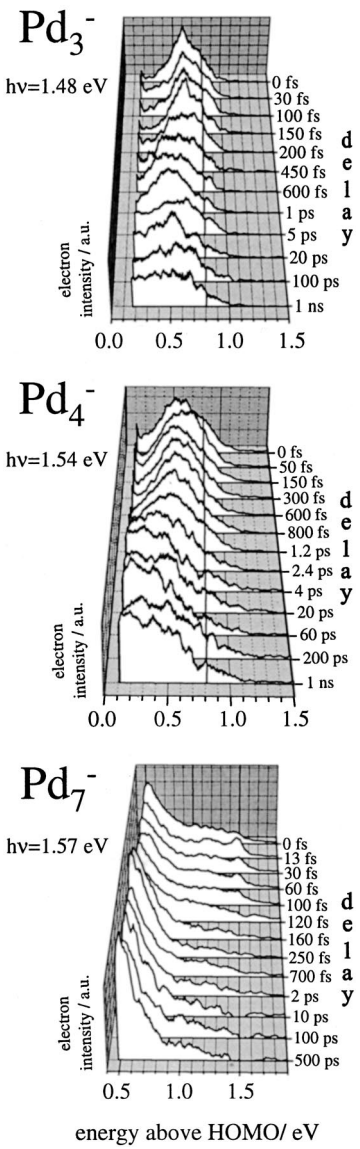

FIG. 1. Pump–probe photoelectron difference spectra of Pd_3^-, Pd_4^-, and Pd_7^- using laser pulses (~80 fs) of ~1.5 eV photon energy. The energy scale refers to the energy of the HOMO which defines the detachment threshold (1.5 eV for Pd_3^-, 1.45 eV for Pd_4^-, and 1.9 eV for Pd_7^-). Each spectrum is normalized to the total intensity to demonstrate the relative intensity changes. Note, however, that the total intensity decreases with increasing delay as shown in Fig. 2.

III. RESULTS AND DISCUSSION

Figure 1 shows a series of pump–probe spectra of Pd_3^-, Pd_4^-, and Pd_7^- which have been recorded with two fs-pulses at ~1.5 eV photon energy. A photon of the first pulse pumps an electron from an occupied to an unoccupied orbital below the detachment threshold. Subsequently an electron of the photoexcited cluster anion is detached by the probe photon leaving the cluster in a neutral final state. The electron dynamics of the initially photoexcited state is studied by delaying the probe pulse with respect to the pump pulse. Each delay spectrum in Fig. 1 is the result of subtracting the intensity of both the pump-only and probe-only spectrum, respectively, from the pump–probe spectrum. Due to saturation effects in the pump step, only 70% of the probe-only spectrum has been subtracted to avoid negative intensities.

As a function of the delay a redistribution of the spectral weight from higher to lower energies is observed for all three palladium clusters in Fig. 1. At zero delay Pd_3^- and Pd_4^- show a broad asymmetric single feature between 0.3 and 1.0 eV. After 1 ps the intensity increases considerably within the lower energy region. After a delay of 5 ps the intensity reaches a maximum value above 0.3 eV while the intensity on the high energy edge is continuously reduced. At a delay of >5 ps the intensity distribution is more or less constant indicating a quasisteady state. The final distribution resembles a steplike function, increasing from zero intensity at 1.0 eV to a flat maximum at <0.7 eV for Pd_3^- and <0.5 eV for Pd_4^-. Although the electron detachment spectrum of Pd_7^- differs distinctly from that of the trimer and tetramer a qualitatively similar time-dependence is revealed: The electron intensity at high energies (0.9–1.6 eV) drops continuously while the intensity below 0.9 eV rises correspondingly within the first ps after excitation. The intensity in the final spectrum at 500 ps increases roughly exponentially towards the HOMO.

Generally, the dynamics of the three Pd-clusters can be explained in terms of inelastic scattering of the excited hot electrons. Thereby the initially excited electron–hole pair relaxes into levels of lower excitation energies under simultaneous creation of secondary electron–hole pairs. Such inelastic scattering processes will maximize the internal entropy and result in multielectron excitations. Note that the total excitation energy $h\nu$ is conserved in the free cluster so that all intermediate states have to be degenerate at the same total energy of the system.

In general the inelastic scattering rate of an electron is given by $1/\tau = 1/\tau_{e-e} + 1/\tau_{e-\mathrm{nucl}}$. Here τ_{e-e} is the effective scattering lifetime due to electron–electron interaction and $\tau_{e-\mathrm{nucl}}$ is the time constant for the energy transfer from the electronic system to nuclear degrees of freedom. In order to extract the relaxation time for the optically excited electrons we have applied a first order rate equation for the population $N(t)$ of the initially excited electrons $dN(t)/dt = A(t) - \beta N(t)$, where $A(t)$ is proportional to the temporal envelope of the pump pulse and β is the inverse lifetime $1/\tau$.[18] As this first order rate equation is fulfilled only for a pure decay dynamics without refilling cascade processes we have applied the fit only to the population dynamics of the highest excited electrons: for Pd_3^- and Pd_4^- from 0.8 to 1.5 eV above the HOMO, and for Pd_7^- from 1.1 to 1.6 eV.[19] These intervals cover the leading feature of each spectrum. The photoelectron intensity $P(\Delta t)$ as a function of the time delay Δt is proportional to the integral of the electron population $N(t)$ times the temporal intensity distribution of the probe pulse $I(t)$: $P(\Delta t) \propto \int_{-\infty}^{\infty} I(t-\Delta t) \cdot N(t) dt$.[18] Approximating the transient population $N(t)$ by a first order rate equation, $P(\Delta t)$ has been fitted (straight line) to the data (open circle) from zero to 2 ps in order to deduce the effective electron relaxation lifetime τ_{e-e}. The corresponding fits are shown in Fig. 2 from which the effective lifetimes τ have been derived: (42 ± 19) fs for Pd_3^-, (91 ± 17) fs for Pd_4^-, and (25 ± 14) fs for Pd_7^-. Note that the data points (filled circle) above 2 ps are systematically positioned below the fitted curve. This is because the electron yield originating from the

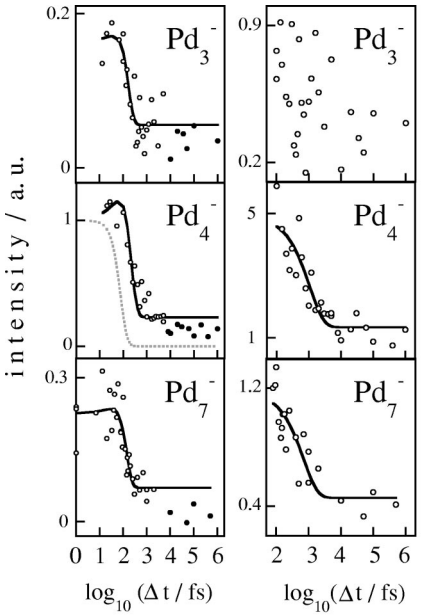

FIG. 2. (Left) the integrated two-photon photoemission intensity from 0.8 to 1.5 eV above the HOMO of Pd_3^- and Pd_4^-, and from 1.1 to 1.6 eV above the HOMO for Pd_7^- as a function of the delay. The dashed curve in the Pd_4^--plot represents a pure autocorrelation trace calculated for 80 fs pulses. The shifts of the falling edges of the fit curves with respect to the autocorrelation trace indicate the finite lifetime of the excited electrons. (Right) the total photoelectron yield (0–1.5 eV above the HOMO of $Pd_{3,4}^-$ and 0.4–1.6 for Pd_7^-) as function of the delay. From an exponential fit to the data >100 fs the vibrational relaxation time constant $\tau_{e-\mathrm{nucl}}$ has been fitted for Pd_4^- and Pd_7^-. The decrease is also obvious for Pd_3^- though the data are too noisy for a reliable fit.

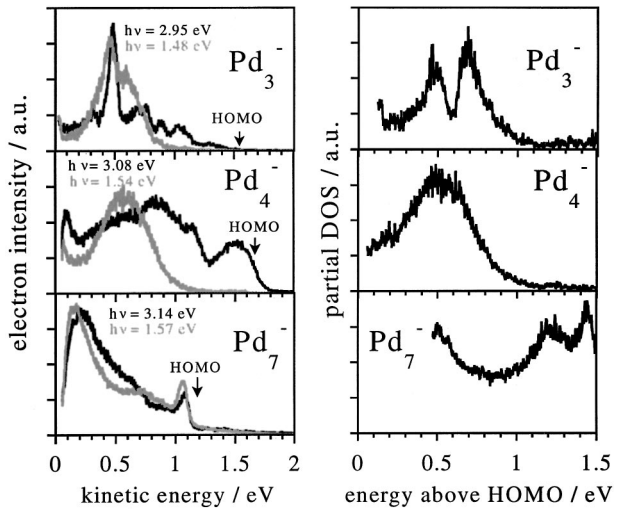

FIG. 3. (Left) photoelectron spectra of Pd_3^-, Pd_4^-, and Pd_7^- recorded with femtosecond pulses at ~3 eV (bold) and ~1.5 eV (faint) photon energy, respectively. The term "HOMO" refers to the maximum kinetic energy of an electron detached with a single photon from the highest occupied molecular orbital. (Right) the partial density of unoccupied states as deduced from dividing the resonant by the direct photoemission spectrum.

equilibrated electron distribution decreases on a long time scale due to an energy flow into the vibrational system (see Fig. 4).

The ultrashort relaxation times (<100 fs) are first of all attributed to electron–electron scattering so that to a good approximation $\tau \sim \tau_{e-e}$. The variation of the relaxation times is most likely caused by differences in the electronic level density of the individual palladium clusters. This is evident from an inspection of the normal (direct) and resonant photoelectron spectra (Fig. 3, left column). Here the 3 eV-spectrum (bold) shows the result by direct photoemission, which is approximately equal to the occupied density of states. The 1.5 eV-spectrum (faint) shows the result of two-photon photoemission via a resonant state. Neglecting any relaxation within the pulsewidth the resonant two-photon photoelectron spectrum probes the joint density of states, from which the partial unoccupied level density $g_p(E_n) = |M_{ni}|^2 g(E_n = E_i + \hbar\omega)$ has been deduced (Fig. 3, right column). Here M_{ni} is the dipole matrix element for the resonant transition of the initial state $|i\rangle$ to the intermediate state $|n\rangle$ and $g(E)$ corresponds to the level density. The occupied level density, on the other hand, is approximately given by the direct photoemission spectrum. We note that our normal photoemission spectra taken with single fs-laser pulses of 3 eV are very similar to the spectra taken with ns-laser pulses at 4 eV;[8] merely the Pd_3^- photoelectron spectrum of Ervin *et al.*[20] shows more fine structure due to a higher electron energy resolution provided by a dispersive spectrometer. The partial unoccupied level density of Pd_7^- is fairly homogeneous up to 1.5 eV above the HOMO while those of Pd_3^- and Pd_4^- vanish at energies larger than 1 eV above the HOMO. This abrupt decrease indicates a cutoff of the *d*-level density. According to Fermi liquid theory the relaxation times decrease the higher the electrons are excited above the Fermi energy. Indeed Pd_7^- shows a faster relaxation than Pd_3^- and Pd_4^- in agreement with the extended unoccupied level density of Pd_7^-. Pd_3^- shows a smaller relaxation time than Pd_4^- even though the former is expected to have a smaller level density. We attribute the larger scattering rate of the trimer to the individual electronic structure which results in a higher degree of quasidegenerate states at 1.5 eV excitation energy.

Note that the *total* two-photon photoelectron intensity decreases with increasing delay time as shown on the right-hand side in Fig. 2. This can be explained by the cooling of the thermalized electron system. Thereby the energy is withdrawn from the electronic system at the expense of an increasing temperature of the vibrational system. As long as the energy drains off into the nuclear system the total number of hot electrons probed in our experiment decreases. The time constant of the vibrational heat transfer $\tau_{e-\mathrm{nucl}}$ has been approximated by an exponential fit to the data at delay times larger than 100 fs where a pure decay (pump pulse width ~80 fs) is assumed. From this we derive an electron-vibrational time constant of (0.7 ± 0.3) ps for Pd_7^- and (1 ± 0.3) ps for Pd_4^-. The energy transfer is faster in Pd_7^- than in Pd_4^- which is consistent with the larger number of vibrational degrees of freedom in the heptamer. The energy transfer to the nuclear system leads to vibrational excitations, isomerization or even to a "melting" of the cluster.[21] Note that dissociation is very unlikely as the dissociation energies of the palladium clusters are larger than 1.5 eV, e.g., for Pd_3 it amounts to 2.3 eV.[22] The experimental results are all listed in Table I.

TABLE I. Experimental inelastic electron relaxation time constants of small Pd_n^--clusters. The excitation energy above the HOMO defines the energy range in which the electron yield has been integrated for the evaluation of τ_{e-e}.

	Pd_3^-	Pd_4^-	Pd_7^-
τ_{e-e}/fs	42±19	91±17	25±14
Excitation energy above HOMO/eV	0,8–1,5	0,8–1,5	1,1–1,6
$\tau_{e-\mathrm{nucl}}$/ps	···	0.7±0.3	1.0±0.3

Assuming a four-atom cluster with 40 valence electrons a qualitative model calculation of the decreasing hot electron yield as a function of temperature is shown in Fig. 4. The nonthermal electron distribution at $\Delta t=0$ simulates the joint density of states assuming equal matrix elements for each transition. Before an appreciable amount of energy is transferred into the vibrational system the energy thermalizes solely within the electronic system ($\Delta t>10^2$ fs). The resulting thermal electron distribution is assumed to be represented by a Fermi function at 1.5 eV internal energy. The population of level n with eigenvalue ε_n is then given by $f_n=1/(e^{(\varepsilon_n-\mu)/k_BT_{\mathrm{el}}}+1)$. T_{el} corresponds to the electronic temperature and k_B is the Boltzmann constant. $\mu(T)$ is equal to the energy at which the Fermi-function f_n is 0.5.[23] In this simulation a mean level spacing of 100 meV is assumed according to the *d*- and *sp*-band width of solid palladium (~4 eV and ~13 eV, respectively) and the number of total valence electrons ($N=40$). From the total internal energy $h\nu=\Sigma_n g_n\varepsilon_n f_n$ an electronic temperature $T_{\mathrm{el}}=3090$ K is derived. The corresponding Fermi distribution is shown in Fig. 4 ($\Delta t>10^2$ fs). In this simulation a fictitious level density has been simulated by taking into account a ground state configuration $d^9s^1p^0$ and a bandwidth of 5 eV for the ''*d*''-levels and 20 eV for the ''*sp*''-levels. Within an energy interval $E_{\mathrm{Fermi}}-1.5$ and $E_{\mathrm{Fermi}}+1.5$ eV, 32 levels (26 occupied, 6 unoccupied) result which are arbitrarily distributed above and below E_{Fermi} to simulate a spectrum. The energy levels have been broadened by a Gaussian (100 meV) to reproduce the vibrational and experimental broadening.

On a long time scale energy drains off the electronic system until thermal equilibrium between the electronic and nuclear system is reached, i.e., at $\Delta t>10^4$ fs as obvious from the experimental data. Taking into account the specific heat of an electron gas and the vibrational system (k_BT_{vib} per vibrational degree of freedom) an equilibrium temperature of 1860 K results (Fig. 4, $\Delta t>10^4$ fs). Note that the total hot electron yield (hatched) clearly decreases in agreement with the experimental result in Fig. 2. Moreover the redistribution of hot electrons from higher to lower energies is nicely reproduced by the simulation.

We attribute the much faster relaxation behavior of small Pd-clusters with respect to simple metal clusters to the drastically enhanced level density. In fact, for Ag and Na clusters with some tens of atoms the level structure is much more discrete than that of Pd and Pt as exhibited by the corresponding photodetachment spectra.[24–26] As the level density grows with increasing cluster size, it is interesting to estimate how much larger a Ag-cluster has to be to achieve a similar level density near ''E_{Fermi}'' as a Pd-cluster. A rough estimate could be derived as follows: The valence level density of Ag near E_{Fermi} is 0.8/eV [four $(s+p)$-levels per atom, bandwidth 20 eV]; that of Pd is 4.8/eV (additional five *d*-levels within a bandwidth of 5 eV). Thus a silver cluster should be six times larger than a palladium cluster to achieve a similar level density and—assuming that the relaxation times depend primarily on the level density—similar electronic relaxation times. From our results we conclude that solid-state like behavior of clusters does not only depend on its size but on the nature of electronic states; tightly bound *d*-states converge much more quickly to a ''band'' than do *s*-levels.

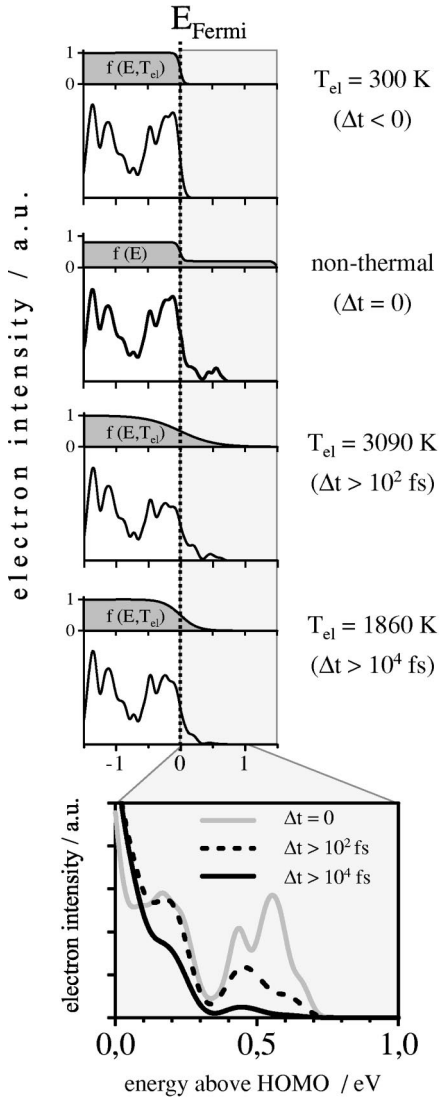

FIG. 4. A qualitative simulation of the decreasing photoelectron yield above the Fermi level assuming a Fermi distribution of the thermalized electrons in ''Pd_4^-''. The hatched area shows the energy region above the HOMO (hot electron region) which is probed in the experiment.

ACKNOWLEDGMENTS

A. Liebsch, Forschungszentrum Jülich GmbH, is gratefully acknowledged for his interest, valuable suggestions, and critical reading of the manuscript. The authors also thank A. Bringer, Forschungszentrum Jülich GmbH, for stimulating discussions.

[1] M. Wolf and G. Ertl, Science **288**, 1352 (2000).
[2] E. Knoesel, A. Hotzel, T. Hertel, M. Wolf, and G. Ertl, Surf. Sci. **368**, 76 (1996).
[3] M. Aeschlimann, M. Bauer, and S. Pawlik, Chem. Phys. **205**, 127 (1996).
[4] H. Petek and S. Ogawa, Prog. Surf. Sci. **56**, 239 (1997).
[5] J. J. Quinn and R. A. Fevrell, Phys. Rev. **112**, 812 (1958).
[6] E. Zarate, P. Apell, and P. M. Echenique, Phys. Rev. B **60**, 2326 (1999).
[7] D. E. Ellis, J. Guo, H.-P. Cheng, and J. J. Low, Adv. Quantum Chem. **22**, 125 (1991).
[8] G. Ganteför and W. Eberhardt, Phys. Rev. Lett. **76**, 4975 (1996).
[9] H. Wu, S. R. Desai, and L.-S. Wang, Phys. Rev. Lett. **76**, 212 (1996).
[10] C. Voisin, D. Christofilos, N. Del Fatti, F. Vallee, B. Prevel, E. Cottancin, J. Lerme, M. Pellarin, and M. Broyer, Phys. Rev. Lett. **85**, 2200 (2000).
[11] J.-Y. Bigot, J.-C. Merle, O. Cregut, and A. Daunois, Phys. Rev. Lett. **75**, 4702 (1995).
[12] M. Perner, P. Bost, U. Lemmer, G. von Plessen, J. Feldmann, U. Becker, M. Mennig, M. Schmitt, and H. Schmidt, Phys. Rev. Lett. **78**, 2192 (1997).
[13] A. Liebsch, Phys. Rev. B **48**, 11317 (1993).
[14] A. Liebsch, Phys. Rev. Lett. **71**, 145 (1993).
[15] C. L. Bastidas, J. A. Maytorena, and A. Liebsch, Phys. Rev. Lett. (in press).
[16] N. Pontius, P. S. Bechthold, M. Neeb, and W. Eberhardt, Appl. Phys. B: Lasers Opt. **71**, 351 (2000).
[17] C. Y. Cha, G. Ganteför, and W. Eberhardt, Rev. Sci. Instrum. **63**, 5661 (1992).
[18] N. Pontius, P. S. Bechthold, M. Neeb, and W. Eberhardt, Phys. Rev. Lett. **84**, 1132 (2000).
[19] The small intensity between 1.6 and 1.9 eV in the spectrum of Pd_7^- arises from three-photon processes and has not been considered in the integration.
[20] K. M. Ervin, J. Hoe, and W. C. Lineberger, J. Chem. Phys. **89**, 4514 (1988).
[21] J. Akola, M. Manninen, H. Hakkinen, U. Landman, Xi Li, and L.-S. Wang, Phys. Rev. B **60**, R11297 (1999).
[22] V. A. Spasov and K. M. Ervin, J. Chem. Phys. **109**, 5344 (1998).
[23] In the thermodynamic limit $\mu(T)$ is the chemical potential which is equal to the Fermi energy at $T=0$. Note that f_n is valid for any kind of Fermi system, regardless whether the electronic states are distributed in a continuous or discrete pattern. μ has been calculated from the total number of valence electrons (N) due to the constraint $\Sigma_n g_n f_n = N$, where g_n is the degeneracy of level n.
[24] K. M. McHugh, J. G. Eaton, G. H. Lee, H. W. Sarkas, L. H. Kidder, J. T. Snodgrass, M. R. Manaa, and K. H. Bowen, J. Chem. Phys. **91**, 3792 (1989).
[25] H. Handschuh, C. Y. Cha, P. S. Bechthold, G. Ganteför, and W. Eberhardt, J. Chem. Phys. **102**, 6406 (1995).
[26] G. Ganteför, H. Handschuh, H. Möller, C. Y. Cha, P. S. Bechthold, and W. Eberhardt, Surf. Rev. Lett. **3**, 399 (1996).